A variational quantum algorithm for the uncapacitated facility location problem

Sha-Sha Wang ¹, Hai-Ling Liu ¹, Fei Gao ¹,* Su-Juan Qin ¹,[†] and Qiao-Yan Wen ^{1‡}

¹ State Key Laboratory of Networking and Switching Technology,

Beijing University of Posts and Telecommunications, Beijing 100876, China

(Dated: December 13, 2023)

The Quantum Alternating Operator Ansatz (QAOA+) is one of the Variational Quantum Algorithms (VQAs) for solving combinatorial optimization problems, which searches for a target solution in the feasible space of the constrained optimization problems. However, the performance of QAOA+ may be influenced by the presence of unconstrained variables of the constrained optimization problems. For simplicity, we call them as Include-Unconstrained-Variables-Problems (IUVPs). Considering Hardware-Efficient Ansatz (HEA) has the advantage of minimizing circuit depth and being easy to implement efficiently on a quantum chip. In this paper, taking the Uncapacitated Facility Location Problem (UFLP) as an example, we leverage the benefits of QAOA+ and HEA to develop an ansatz named HE-QAOA+ for addressing IUVPs. One of the cores of this algorithm is the construction of mixed Hamiltonian. To facilitate the creation of the mixed Hamiltonian, we transform UFLP into a constrained optimization problem belonging to IUVPs, where the feasible space is composed of bit strings with a fixed Hamming weight. Finally, the numerical results demonstrate that HE-QAOA+ has a significantly higher success probability at lower circuit depths compared to the Quantum Approximation Optimization Algorithm (QAOA), QAOA+, and HEA. The proposed algorithm offers a viable solution for addressing the IUVPs, inspiring the development of other approaches for tackling analogous problems.

I. INTRODUCTION

By harnessing quantum effects, quantum computers offer computational advantages over classical computers, delivering polynomial or even exponential speedups for specific problems, such as integer factorization [1], unstructured data search [2], linear regression [3, 4], quantum error correction [5], matrix computation [6–9], and cryptanalysis [10]. However, the current quantum hardware devices only support a limited number of physical qubits and limited gate fidelity, which makes the above quantum algorithms unable to be implemented on near-term devices.

Variational quantum algorithms (VQAs) are a hot class of hybrid quantum-classical algorithms, with the core being the design of ansatz, which are expected to realize quantum advantages on Noisy Intermediate-Scale Quantum (NISQ) devices [11, 12]. Ansatz is generally divided into two types: problem-agnostic ansatz and problem-inspired ansatz. The structure of the problemagnostic ansatz carries no information about the problem itself and is mostly suited for optimization problems, such as the Hardware-Efficient Ansatz (HEA) [13], which has the advantage of reducing the circuit depth as much as possible and being easy to implement efficiently on a quantum chip. The specific structure of the problem-inspired ansatz typically depends on the task at hand, such as Quantum Alternating Operator Ansatz (QAOA+) [19], which has the advantage of preserving the feasible subspace, resulting in the complete

elimination of invalid solutions, and has been also applied to many combinatorial optimization problems [20–24]. However, the performance of QAOA+ may deteriorate when applied to constrained optimization problems involving unconstrained variables. For simplicity, we call such problems as Include-Unconstrained-Variables-Problems (IUVPs). To address the IUVPs, we propose a hybrid approach that leverages the strengths of both HEA and QAOA+.

The Uncapacitated Facility Location Problem (UFLP) [25] is one of the most important NP-hard problems, and can be transformed into a variant of IUVPs. In this paper, taking the UFLP as an example, we propose a combined ansatz termed HE-QAOA+ for IUVPs. Similar to QAOA+, the circuit consists of p alternating layers of the phase-separation operator and the mixing operator applied to an initial state. The mixing operator will preserve the feasible space (the space composed of feasible solutions), and the initial state is required to be a trivial feasible state (the quantum state corresponding to a trivial feasible solution). The algorithm can limit the state of the system to the feasible space, resulting in zero probability of obtaining invalid solutions. Different from QAOA+, its alternating operators act on different qubits separately, which can be parallelized.

In particular, UFLP is a linear programming problem whose mathematical model contains an inequality constraint, to facilitate solving the problem, we transform the inequality constraint into equality constraint by introducing slack variables. To facilitate the construction of a mixed Hamiltonian, a penalty function approach is adopted by including a constraint as part of the objective function, resulting in a novel constrained optimization problem belonging to IUVPs, where the feasible space is composed of bit strings with a fixed Hamming weight 1.

^{*} gaof@bupt.edu.cn

[†] qsujuan@bupt.edu.cn

 $^{^{\}ddagger}$ wqy@bupt.edu.cn

To verify the efficiency of the algorithm, we simulate it for UFLP with 12 instances by using MindQuantum [33], showing that it has lower circuit depth and higher success probability at the same low-layer p compared to the QAOA, QAOA+, and HEA. Moreover, our algorithm reduces the number of CNOT gates and parameter gates by at least 53% and 59% compared to QAOA and QAOA+, respectively, and the number of parameters by at least 33% compared to HEA.

This paper is organized as follows. In Sec. II, the HE-QAOA+ algorithm is proposed. In Sec. III, we apply HE-QAOA+ to solve IUVPs. In Sec. IV, numerical results and analysis are given. Finally, the conclusion is given in Sec. V.

II. HE-QAOA+

In QAOA+ [19], the variational ansatz consists of p layers, each containing a phase separator Hamiltonian H_P and a mixer Hamiltonian H_M :

$$|\psi_p(\overrightarrow{\gamma}, \overrightarrow{\beta})\rangle = U(H_M, \beta_p)U(H_P, \gamma_p) \cdots U(H_P, \gamma_1)|x\rangle,$$
(1)

where $U(H_M, \beta_j) = e^{-i\beta_j H_M}$, $U(H_P, \gamma_j) = e^{-i\gamma_j H_P}$, $j = 1, 2, \cdots, p$, and the initial state $|x\rangle$ is a trivial feasible solution, or the uniform superposition state of trivial feasible solutions, and $\overrightarrow{\gamma} = (\gamma_1, \gamma_2, \cdots, \gamma_p)$ and $\overrightarrow{\beta} = (\beta_1, \beta_2, \cdots, \beta_p)$ are variational parameters sets. The variational parameters are optimized on classical computer with the goal of finding the optimal parameters $(\overrightarrow{\gamma^*}, \overrightarrow{\beta^*})$, which are obtained by minimizing the expected value of the phase separator Hamiltonian H_P

$$(\overrightarrow{\gamma^*}, \overrightarrow{\beta^*}) = arg \min_{\overrightarrow{\gamma}, \overrightarrow{\beta}} F_p(\overrightarrow{\gamma}, \overrightarrow{\beta}),$$
 (2)

where $F_p(\overrightarrow{\gamma}, \overrightarrow{\beta}) = \langle \psi_p(\overrightarrow{\gamma}, \overrightarrow{\beta}) | H_P | \psi_p(\overrightarrow{\gamma}, \overrightarrow{\beta}) \rangle$.

A family of mixing operators $U(H_M,\beta)$ of QAOA+ limits the state of the system to the feasible space, and results in zero probability of obtaining invalid solutions, which is the advantage of the algorithm. In contrast, a family of phase-separation operators $U(H_P,\gamma)$ of QAOA+ only changes the phase and has no significant effect on the result [21]. Moreover, $U(H_P,\gamma)$ always introduces a lot of CNOT and R_Z gates, increasing circuit depth. HEA has the advantage of reducing the circuit depth as much as possible and being easy to implement efficiently on a quantum chip [13]. For IUVPs, to reduce the circuit depth, we consider performing HEA [13] on non-constrained variables.

In this work, we replace the $U(H_P, \gamma)$ with the unitary operator $U_{HEA}(\gamma)$ of HEA

$$|\psi_p(\overrightarrow{\gamma}, \overrightarrow{\beta})\rangle = U(H_M, \beta_p)U_{HEA}(\overrightarrow{\gamma_p}) \cdots U_{HEA}(\overrightarrow{\gamma_1})|x\rangle,$$
(3)

where $\overrightarrow{\gamma_i} = (\gamma_i^1, \gamma_i^2, \cdots, \gamma_i^l)$, $i = 1, 2, \cdots, p$, and l is the number of non-constrained variables. $U(H_M, \beta_i)$ acts on variables of the constraints, and $U_{HEA}(\overrightarrow{\gamma_i})$ acts on non-constrained variables in constrained optimization problems. This algorithm is designed for IUVPs, which we call HE-QAOA+. The crucial points of HE-QAOA+ are the initial state $|x\rangle$, the mixing operators $U(H_M, \beta)$, the unitary operators $U_{HEA}(\gamma)$, and the phase separator Hamiltonian H_P . The framework of the HE-QAOA+ is shown in Figure 1.

To evaluate the quality of the solution for the optimization problem, we define the success probability as the probability of finding the optimal solution

$$P_{success} = |\langle x_{sol} | \psi_p(\overrightarrow{\gamma}, \overrightarrow{\beta}) \rangle|^2, \tag{4}$$

where x_{sol} is an optimal solution to the problem.

III. APPLY HE-QAOA+ TO SOLVE IUVPS

The UFLP is a combinatorial optimization problem that can be transformed into a variant of IUVPs. In this section, we first introduce the definition and the mathematical model of UFLP. Then, we solve UFLP using HE-QAOA+.

A. UFLP

The UFLP [25] first proposed in 1963, is one of the most important NP-hard problems in location theory [26]. Currently, UFLP has significant applications in the fields of resource allocation [27], logistics and transportation [28], computer networks [29], and computer vision [30]. Over the past decades, many classic methods [31, 32] have been proposed to solve UFLP. However, there still exists a research gap in the field of quantum algorithms for addressing this particular issue.

The definition of UFLP is generally described as [32]: giving the set $K = \{k_1, \cdots, k_m\}$ of customers, where m is the number of customers and k_i is the ith customer. Giving the set $S = \{s_1, \cdots, s_n\}$ of potential facilities that can be opened, where n is the number of facilities and s_j is the jth facility. Giving an $m \times n$ matrix $D = [d_{ij}]_{m \times n}$, where d_{ij} represents the service cost when the ith customer receives the service from the jth facility. $G = \{g_1, \cdots, g_n\}$ is the set of fixed open cost of facilities, where g_j represents the opening cost required by the opening of the jth facility. It is worthy to note that the demand of any customer is fulfill by only one facility. The goal of UFLP is to find a set of open facilities and a reasonable allocation scheme between facilities and customers, so that the sum of total service costs and total open facility costs is minimized.

The mathematical model of UFLP [32] is described as

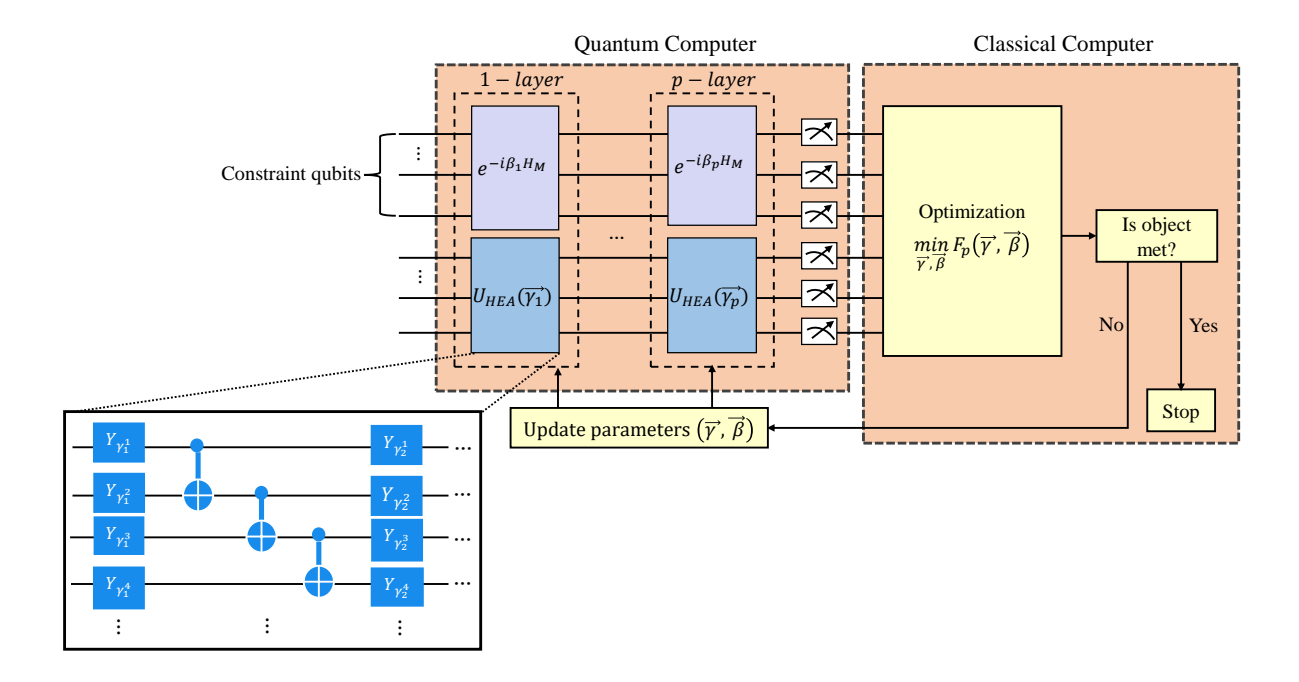


FIG. 1. The framework of the HE-QAOA+. The variational parameters were optimized on a classical computer, and a quantum computer was used to evaluate the expected value of the objective function. The mixing operator $U(H_M, \beta_i)$ acts on variables of the constraints, and the unitary operator $U_{HEA}(\overrightarrow{\gamma_i})$ of HEA acts on non-constrained variables in the constrained optimization problems.

follows

$$min \quad \sum_{i=1}^{m} \sum_{j=1}^{n} d_{ij} y_{ij} + \sum_{j=1}^{n} g_{j} x_{j}, \tag{5}$$

s.t.
$$\sum_{i=1}^{n} y_{ij} = 1, \quad i = 1, 2, \dots, m,$$
 (6)

$$y_{ij} \le x_j, \quad i = 1, 2, \dots, m, j = 1, 2, \dots, n,$$
 (7)

$$y_{ij}, x_j \in \{0, 1\},$$
 (8)

where $y_{ij} = 1$ if *i*th customer gets service from *j*th facility; otherwise $y_{ij} = 0$, and $x_j = 1$ if *j*th facility is opened; otherwise $x_j = 0$. The number of binary decision variables is mn + n. The first term in the Eq. (5) denotes the total service cost, and the second term denotes the total opening cost of the opened facilities. The Eq. (6) ensures that every customer is served by exactly one facility. The Eq. (7) ensures that a customer can be served from a facility only if a facility is opened.

To facilitate solving UFLP, we transformed the above optimization problem into the following standard form

by introducing slack variables z_{ij}

$$min \quad \sum_{i=1}^{m} \sum_{j=1}^{n} d_{ij} y_{ij} + \sum_{j=1}^{n} g_{j} x_{j}, \tag{9}$$

s.t.
$$\sum_{i=1}^{n} y_{ij} = 1, \quad i = 1, 2, \dots, m,$$
 (10)

$$y_{ij} + z_{ij} - x_j = 0, \quad i = 1, \dots, m, j = 1, \dots, n,$$
(11)

$$z_{ij}, y_{ij}, x_j \in \{0, 1\}. \tag{12}$$

The number of binary decision variables is 2mn + n.

HE-QAOA+ encodes constraints directly into quantum circuits, limiting the state of the system to the feasible space, which implies a significant advantage compared to these algorithms. However, one of the cores of this algorithm is the construction of mixed Hamiltonian.

To facilitate the creation of a mixed Hamiltonian, we adopt the penalty function approach by making the constraint Eq. (11) a part of the objective function Eq. (9), resulting in the following new optimization problem

$$min \quad \sum_{i=1}^{m} \sum_{j=1}^{n} d_{ij} y_{ij} + \sum_{j=1}^{n} g_j x_j + \lambda h(x, y, z), \quad (13)$$

s.t.
$$\sum_{j=1}^{n} y_{ij} = 1, \quad i = 1, 2, \dots, m,$$
 (14)

$$z_{ij}, y_{ij}, x_j \in \{0, 1\},$$
 (15)

where $h(x, y, z) = \sum_{i=1}^{m} \sum_{j=1}^{n} (y_{ij} + z_{ij} - x_j)^2$, λ is the penalty, determined empirically. The number of constraint variables in Eq. (14) is mn, and the number of non-constrained variables in Eq. (13) is mn+n. Next, we will solve the UFLP via HE-QAOA+ designed in section II.

B. HE-QAOA+ FOR UFLP

The crucial points of HE-QAOA+ are the initial state $|x\rangle$, the mixing operators $U(H_M,\beta)$, the unitary operators $U_{HEA}(\gamma)$, and the phase separator Hamiltonian H_P for UFLP. For initial state $|x\rangle$, according to Eq. (14), the state

The mixing operators $U(H_M, \beta) = e^{-i\beta H_M}$ depend on Eq. (14) and its structure, and its core is to construct H_M . To maintain the Hamming weight 1 of the constraint Eq. (14), the mixing Hamiltonian H_M is expressed as follows [19, 20]

$$H_M = \sum_{i=0}^{m-1} \sum_{j=0}^{n-2} X_{j+i\cdot n} X_{j+i\cdot n+1} + Y_{j+i\cdot n} Y_{j+i\cdot n+1}, \quad (16)$$

where X, and Y represents Pauli-X operation, and Pauli-Y operation respectively.

The unitary operators $U_{HEA}(\gamma)$ of HEA consist of single-qubit rotating gates and entangled gates as shown in Figure 1. The phase separator Hamiltonian H_P is obtained by replacing binary variables x, y, z in Eq. (13) with $\frac{I-Z}{2}$

$$H_{P} = \sum_{i=1}^{m} \sum_{j=1}^{n} d_{ij} \frac{I - Z_{n*(i-1)+j-1}}{2} + \sum_{j=1}^{n} g_{j} \frac{I - Z_{m*n+j-1}}{2} + \lambda \sum_{i=1}^{m} \sum_{j=1}^{n} \left(\frac{I - Z_{n*(i-1)+j-1}}{2} + \frac{I - Z_{n*(m+i)+j-1}}{2} - \frac{I - Z_{m*n+j-1}}{2} \right)^{2}, \tag{17}$$

where Z represents Pauli-Z operation and the subscript represents the qubit of action. After the three key points are structured, we apply HE-QAOA+ to solve the UFLP and perform numerical simulation experiments.

IV. NUMERICAL SIMULATION

In this section, we perform numerical experiments using the MindSpore Quantum [33]. We study 12 instances for three different problem sizes of the UFLP given in Table I to benchmark the performance of HE-QAOA+. Details of the instances are given in Appendix A, corresponding to 10, 14, and 22 qubits, respectively. To

find the optimal variational parameters, an Adam optimizer [34] is utilized which is updated with gradients by an adaptive moment estimation algorithm. For the selection of initial parameters, the random initialization method is adopted.

TABLE I. The instances of UFLP.

$m \times n$	Qubit	Instances	Optimal Value
		Instance 1	16
		Instance 2	42
2×2	10	Instance 3	30
		Instance 4	39
		Instance 5	52
	14	Instance 6	21
		Instance 7	42
3×2		Instance 8	40
		Instance 9	35
		Instance 10	43
5×2	22	Instance 11	82
3 × Z		Instance 12	95

To verify the high efficiency of HE-QAOA+, we also apply QAOA, QAOA+, and HEA to UFLP and compared them, giving the Hamiltonians and the corresponding circuits, as specified in Appendix B, C, and D respectively. In Fig. 2, we performed numerical simulations up to p=6 using random initialization for 12 instances. The circuit depth and average success probability as a function of the layers are shown for the standard QAOA, QAOA+, HEA, and HE-QAOA+, respectively.

Specifically, for m = 2, n = 2, in Fig. 2 (a) and (b), HE-QAOA+ has a higher success probability than the other three algorithms, at least 54% higher. Meanwhile, HE-QAOA+ has the same circuit depth as HEA, which is at least 75% lower than QAOA and QAOA+. For m=3, n=2, in Fig. 2 (c) and (d), HE-QAOA+ hasa success probability of at least 58% higher compared to the other three algorithms. Moreover, the circuit depth of HE-QAOA+ is about 26% lower than HEA, and at least 83% lower than QAOA and QAOA+. For m = 5, n = 2, in Fig. 2 (e) and (f), compared to the other three algorithms, HE-QAOA+ has at least five times higher success probability. And, the circuit depth of HE-QAOA+ is about 43% lower than HEA, and at least 87% lower than QAOA and QAOA+. We find that the success probability of HE-QAOA is higher than the other three algorithms by an increasing percentage as the number of qubits increases. Directly, we conjecture that the performance of this algorithm is less affected by the increase in qubits than QAOA, QAOA+ and HEA.

The results show that HE-QAOA+ achieves a significantly higher success probability at low circuit depths compared to the QAOA, QAOA+, and HEA. One of the keys to these four algorithms is to construct the phase separator Hamiltonian. In QAOA and HEA, for constrained optimization problems, the common method is to incorporate hard constraints into the target function as a penalty item, and then convert the target function into a phase separator Hamiltonian [18]. These two al-

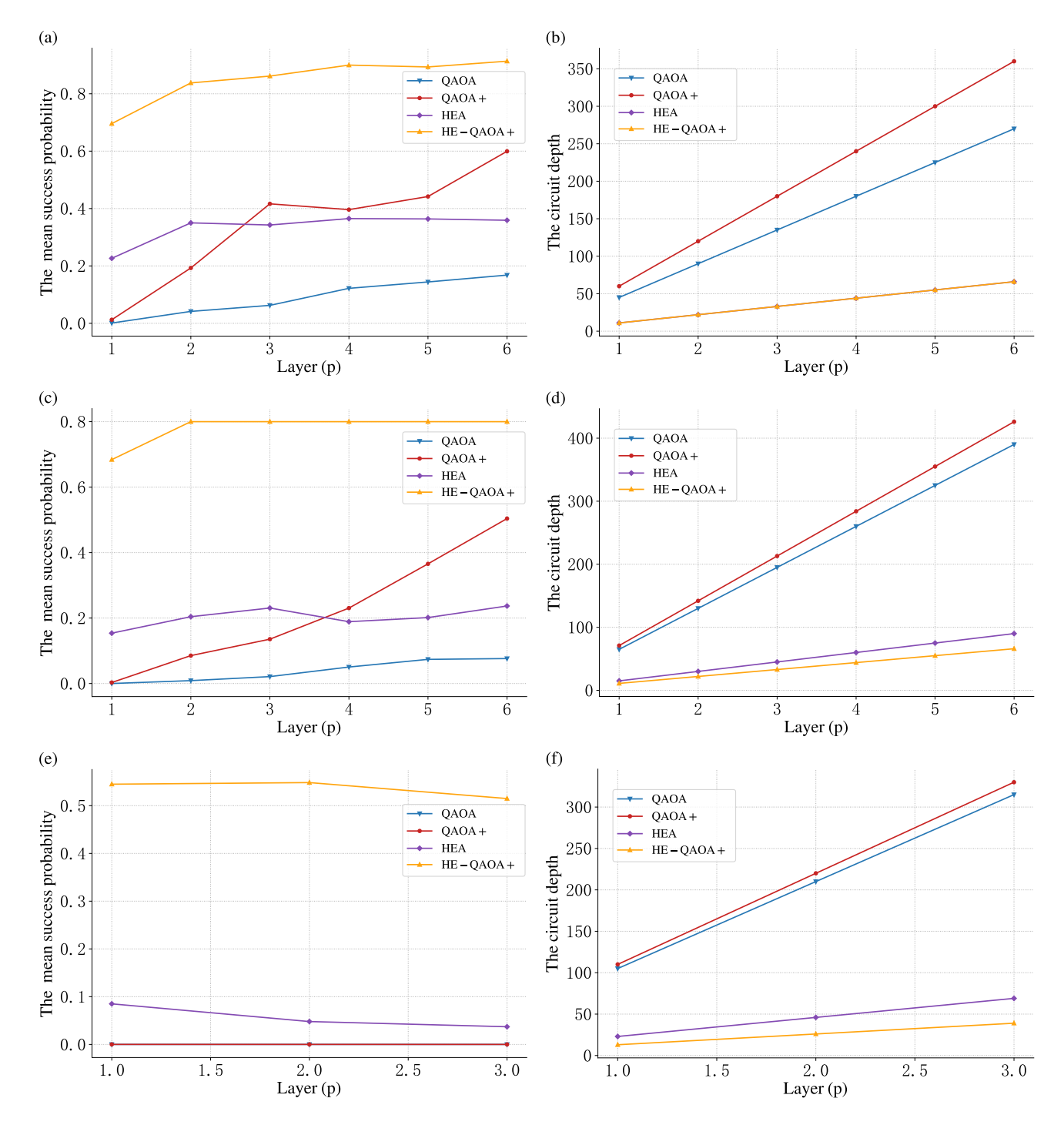


FIG. 2. Comparison of the performance of standard QAOA, QAOA+, HEA, and HE-QAOA+ for the UFLP with 12 instances. The circuit depth and the average success probability as a function of the layers are shown for the standard QAOA, QAOA+, HEA, and HE-QAOA+. (a)-(f) The optimization trajectories from optimizer Adam are plotted versus the number of circuit evaluations. For both cases m=2, n=2 and m=3, n=2, we perform numerical simulations up to p=6 using random initialization. However, owing to the large number of qubits and high circuit depth involved in case m=5, n=2, only simulations from p=1 to p=3 are performed. (a)-(b) m=2, n=2, (c)-(d) m=3, n=2, (e)-(f) m=5, n=2.

gorithms need to search for the target solutions in the Overall Hilbert Space [19]. Differently, HE-QAOA+ encodes the constraints directly into quantum circuits, limiting the state of the system to the Feasible Space (a

subspace of the entire Hilbert space) of the constrained optimization problems, which implies a higher probability of searching a solution compared to these two algorithms. Furthermore, for the Eq. (13) with non-

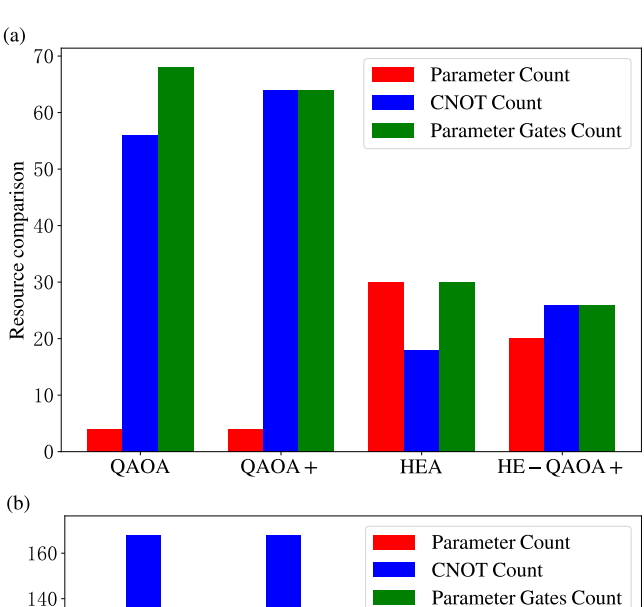
constrained variables, the performance of QAOA+ may deteriorate by the presence of unconstrained variables. QAOA+ performs single-qubit rotating gates R_X and the phase-separation operators $U(H_P, \gamma)$ for non-constrained variables (see Appendix C for details). Among them, the phase-separation operators $U(H_P, \gamma)$ only change the phase as well, contributing much less to the search for a solution than R_X . Besides, $U(H_P, \gamma)$ always introduces a lot of CNOT and R_Z gates, increasing circuit depth. Different from QAOA+, HE-QAOA+ performs HEA consisting of single-qubit rotating gates R_Y and entanglement gates for non-constrained variables (see Fig. 1, where HEA ansatz see Appendix D for details), which has the advantage of reducing the circuit depth as much as possible. Moreover, HE-QAOA+ discards the phase-separation operators $U(H_P, \gamma)$, and its alternating operators act on different qubits separately, which can be parallelized. Therefore, HE-QAOA+ has lower circuit depth and higher success probability at the same low-layer p compared to the standard QAOA, QAOA+, and HEA.

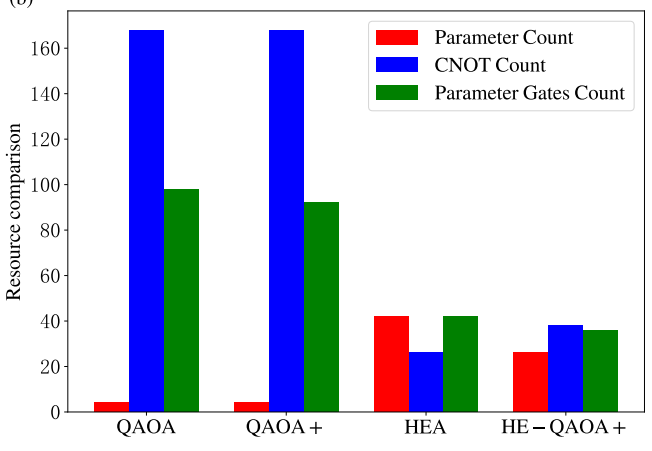
A crucial question, especially for near-term devices, is how the different algorithms compare with respect to resource overhead. We compare quantum resources in terms of the number of CNOT gates, parameter gates, and parameters. Fig. 3 shows the number of parameters, CNOTs, and parameter gates for the four algorithms with p = 2. The results show that our algorithm reduces both the number of CNOT gates by at least 53% and parameter gates by at least 59% compared to QAOA and QAOA+, and the number of parameters by at least 33% and parameter gates by at least 13% compared to HEA. However, our algorithm has significantly more parameters than QAOA and QAOA+, and more CNOT gates than HEA. In other words, the HE-QAOA+ obtains better performance in UFLP at the cost of introducing more variational parameters and CNOTs.

V. CONCLUSION

In conclusion, we proposed HE-QAOA+ for solving IUVPs, a combined ansatz that incorporates the advantages of HEA and QAOA+. To verify the high efficiency of HE-QAOA+, we also applied QAOA, QAOA+, and HEA to UFLP, as well as compare the performance of these four algorithms. The Hamiltonians and the corresponding circuits are given as specified in Appendix B, C, and D respectively. We tested the performance of several instances of UFLP with 10, 14, and 22 qubits, details of the instances are given in Appendix A, finding that HE-QAOA+ always outperforms the other three algorithms (see Fig. 2 for details).

Specifically, for m=2, n=2, in Fig. 2 (a) and (b), HE-QAOA+ has a higher success probability than the other three algorithms, at least 54% higher. Meanwhile, HE-QAOA+ has the same circuit depth as HEA, which is at least 75% lower than QAOA and QAOA+. For





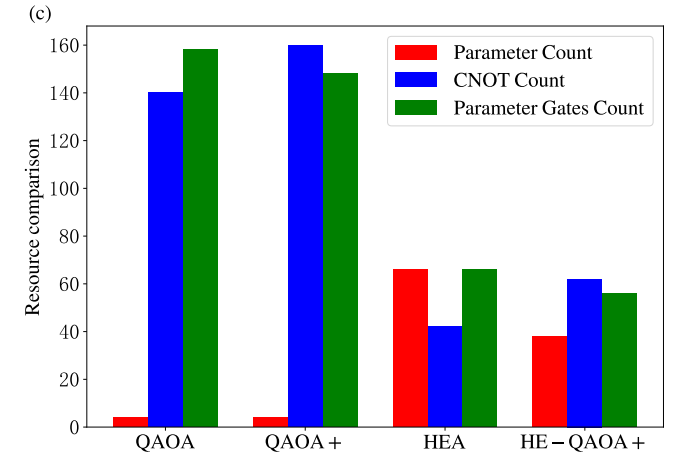


FIG. 3. Resource comparison of the standard QAOA, QAOA+, HEA, and HE-QAOA+ for the UFLP with three different sizes. (a), (b), and (c) show the comparison of four algorithms for the 10, 14, and 22 qubits, respectively.

m=3, n=2, in Fig. 2 (c) and (d), HE-QAOA+ has a success probability of at least 58% higher compared to the other three algorithms. Moreover, the circuit depth of HE-QAOA+ is about 26% lower than HEA, and at least 83% lower than QAOA and QAOA+. For m=5, n=2, in Fig. 2 (e) and (f), compared to the other three algo-

rithms, HE-QAOA+ has at least five times higher success probability. And, the circuit depth of HE-QAOA+ is about 43% lower than HEA, and at least 87% lower than QAOA and QAOA+. In addition, we also compared the number of CNOT gates, parameter gates, and parameters of these four algorithms, and the results showed that our algorithm reduced the number of CNOT gates and parameter gates compared to QAOA and QAOA+, and both parameters and parameter gates are reduced compared to HEA (see Fig. 3 for details). This work provided

a feasible way for solving IUVPs, and inspired for developing other approaches for such problems.

ACKNOWLEDGMENTS

This work is supported by the Beijing Natural Science Foundation (Grant No. 4222031), the National Natural Science Foundation of China (Grant Nos. 61976024, 61972048, 62272056), and the 111 Project B21049.

- [1] P. W. Shor, Algorithms for quantum computation: Discrete logarithms and factoring, in *Proceedings 35th Annual Symposium on Foundations of Computer Science*, pp. 124-134 (1994).
- [2] L. K. Grover, A fast quantum mechanical algorithm for database search, in *Proceedings of the Twenty-Eighth Annual ACM Symposium on the Theory of Computing*, pp. 212-219 (1996).
- [3] C. H. Yu, F. Gao, C. Liu, D. Huynh, M. Reynolds, and J. Wang, Quantum algorithm for visual tracking, Phys. Rev. A 99, 022301 (2019).
- [4] C. H. Yu, F. Gao, and Y. Q. Wen, An improved quantum algorithm for ridge regression, IEEE Trans. Know. Data Eng. 33 (3), 858-866 (2021).
- [5] H. Wang, Y. Xue, Y. Qu, et al., Multidimensional Bose quantum error correction based on neural network decoder, npj Quantum Inf 8, 134 (2022).
- [6] L. C. Wan, C. H. Yu, S. J. Pan, F. Gao, Q. Y. Wen, and S. J. Qin, Asymptotic quantum algorithm for the Toeplitz systems, Phys. Rev. A 97, 062322 (2018).
- [7] H. L. Liu, S. J. Qin, L. C. Wan, C. H. Yu, S. J. Pan, F. Gao, and Q. Y. Wen, A quantum algorithm for solving eigenproblem of the Laplacian matrix of a fully connected weighted graph, Adv Quantum Technol. 2300031 (2023).
- [8] L. C. Wan, C. H. Yu, S. J. Pan, S. J. Qin, F. Gao, and Q. Y. Wen, Block-encoding-based quantum algorithm for linear systems with displacement structures, Phys. Rev. A 104, 062414 (2021).
- [9] H. L. Liu, C. H. Yu, L. C. Wan, S. J. Qin, F. Gao, and Q. Y. Wen, Quantum mean centering for block-encodingbased quantum algorithm, Physica A: Statistical Mechanics and its Applications 607, 128227 (2022).
- [10] Z. Q. Li, B. B. Cai, H. W. Sun, H. L. Liu, L. C. Wan, S. J. Qin, Q. Y. Wen, and F. Gao, Novel quantum circuit implementation of Advanced Encryption Standard with low costs, Sci. China-Phys. Mech. Astron. 65, 290311 (2022).
- [11] J. Preskill, Quantum computing in the NISQ era and beyond, Quantum 2, 79 (2018).
- [12] J. R. McClean, J. Romero, R. Babbush, and A. Aspuru-Guzik, The theory of variational hybrid quantum-classical algorithms, New J. Phys. 18, 023023 (2016).
- [13] A. Kandala, A. Mezzacapo, K. Temme, M. Takita, M. Brink, J. M. Chow, and J. M. Gambetta, Hardware-efficient variational quantum eigensolver for small molecules and quantum magnets, Nature 549, 242-246 (2017).
- [14] R. Biswas, et al., A NASA perspective on quantum com-

- puting: Opportunities and challenges, Parallel Computing ${\bf 64},\,81\text{-}98$ (2017).
- [15] E. G. Rieffel, D. Venturelli, B. O'Gorman, M. B. Do, E. M. Prystay, and V. N. Smelyanskiy, A case study in programming a quantum annealer for hard operational planning problems, Quantum Information Processing, 14 (1), 1-36 (2015).
- [16] S. Hadfield, On the representation of Boolean and real functions as Hamiltonians for quantum computing, in ACM Transactions on Quantum Computing, pp. 1-21 (2021).
- [17] I. Hen and F. M. Spedalieri, Quantum Annealing for Constrained Optimization, Phys. Rev. Applied 5 (3), 034007 (2016).
- [18] V. Choi, Different adiabatic quantum optimization algorithms for the NP-complete exact cover and 3SAT problems, in *Quantum Information & Computation*, pp. 638-648 (2011).
- [19] S. Hadfield, Z. Wang, B. O'Gorman, E. G. Rieffel, D. Venturelli, and R. Biswas, From the quantum approximate optimization algorithm to a quantum alternating operator ansatz, Algorithms 12 (2), 34 (2019).
- [20] Z. H. Wang, N. C. Rubin, J. M. Dominy, and E. G. Rieffel, XY mixers: Analytical and numerical results for the quantum alternating operator ansatz, Phys. Rev. A 10 (1), 012320 (2020).
- [21] S. S. Wang, H. L. Liu, S. J. Qin, F. Gao, and Q. Y. Wen, Quantum Alternating Operator Ansatz for Solving the Minimum Exact Cover Problem, Physica A: Statistical Mechanics and its Applications 626, 129089 (2023).
- [22] J. Cook, S. Eidenbenz, and A. Brtschi, The Quantum Alternating Operator Ansatz on Max-k Vertex Cover, in APS March Meeting, 65, 1 (2020).
- [23] J. Golden, A. Bärtschi, D. O'Malley, and S. Eidenbenz, The Quantum Alternating Operator Ansatz for Satisfiability Problems, arXiv.2301.11292 (2023).
- [24] M. Fingerhuth, B. Tomá, and C. Ing, A quantum alternating operator ansatz with hard and soft constraints for lattice protein folding, arXiv.1810.13411 (2018).
- [25] A. A. Kuehn and M. J. Hamburger, A heuristic program for locating warehouses. Management Science, 9 (4), 643-666 (1963).
- [26] M. Daskin, L. Snyder, and R. Berger, Facility location in supply chain design, in *Logistics systems: design and optimization*, pp. 39-65 (2003).
- [27] J. D. Armas and A. A. Juan, A biased-randomized algorithm for the uncapacitated facility location problem, in Applied mathematics and computational intelligence, pp.

- 287-298 (2018).
- [28] T. Cura, A parallel local search approach to solving the uncapacitated warehouse location problem, Computers & Industrial Engineering, 59 (4), 1000-1009 (2010).
- [29] N. Lazic, B. J. Frey, and P. Aarabi, Solving the uncapacitated facility location problem using message passing algorithms, Expert Systems with Applications, 9 (6), 429-436 (2010).
- [30] N. Lazic, I. Givoni, P. Aarabi, and B. Frey, FLoSS: Facility location for subspace segmentation, in *IEEE international conference on computer vision*, pp. 825-832 (2009).
- [31] S. Korkmaz and M. S. Kiran, An artificial algae algorithm with stigmergic behavior for binary optimization, Applied Soft Computing, 64, 627-640 (2018).
- [32] F. Z. Zhang, Y. C. He, H. B. Ouyang, and W. B. Li, A fast and efficient discrete evolutionary algorithm for the uncapacitated facility location problem, Expert Systems With Applications 213, 118978 (2023).
- [33] MindQuantum Developer, MindQuantum, version 0.6.0, https://gitee.com/mindspore/mindquantum (2021).

- [34] D. P. Kingma and J. Ba, Adam: A method for stochastic optimization, in *International Conference on Learning Representations (ICLR)*, pp. 1-15 (2015).
- [35] B. T. Gard, L. Zhu, G. S. Barron, N. J. Mayhall, S. E. Economou, and E. Barnes, Efficient symmetry-preserving state preparation circuits for the variational quantum eigensolver algorithm, npj Quantum Information 6, 1-9 (2020).
- [36] M. Otten, C. L. Cortes, and S. K. Gray, Noise-resilient quantum dynamics using symmetry-preserving ansatzes, arXiv:1910.06284 (2019).
- [37] N. V. Tkachenko, J. Sud, Y. Zhang, S. Tretiak, P. M. Anisimov, A. T. Arrasmith, P. J. Coles, L. Cincio, and P. A. Dub, Correlation-informed permutation of qubits for reducing ansatz depth in VQE, PRX Quantum 2, 020337 (2021).
- [38] C. Kokail, C. Maier, R. V. Bijnen, T. Brydges, M. K. Joshi, P. Jurcevic, C. A. Muschik, P. Silvi, R. Blatt, C. F. Roos, et al., Self-verifying variational quantum simulation of lattice models, Nature 569, 355-360 (2019).

Appendix A: Details of instances

In section $\,$ IV, numerical simulations are performed for 12 instances as shown in Table $\,$ II, Table $\,$ III, and Table $\,$ IV.

TABLE II. The Instance 1-Instance 5 of UFLP.

$m \times n$	Qubit	The service matrix D	The set G of fixed open cost of facilities	Optimal Value
		$\begin{bmatrix} 6 & 10 \\ 3 & 5 \end{bmatrix}$	{7,7}	16
		$\begin{bmatrix} 16 & 10 \\ 13 & 15 \end{bmatrix}$	{17, 17}	42
2×2	10	$\begin{bmatrix} 8 & 15 \\ 20 & 15 \end{bmatrix}$	$\{9, 10\}$	30
		$\begin{bmatrix} 6 & 20 \\ 13 & 25 \end{bmatrix}$	$\{20, 20\}$	39
		$\begin{bmatrix} 25 & 20 \\ 6 & 17 \end{bmatrix}$	$\{27, 15\}$	52

Appendix B: QAOA for UFLP

The general framework of QAOA is similar to QAOA+ as shown in section II, which we will not review here. Similarly, the crucial points of QAOA are the initial state $|x\rangle$, the mixing operators $U(H_M,\beta)$, and the phase-separation operators $U(H_P,\gamma)$ for UFLP. The initial state is generally chosen as a uniform superposition state, i.e. $|+\rangle^{\bigotimes N}$, N=2mn+n. For the mixing operators $U(H_M,\beta)=e^{-i\beta H_M}$, and its core is to construct H_M , where H_M

TABLE I	III The	Instance	6-Instance	10 of UFLP.

$m \times n$	Qubit	The service matrix D	The set G of fixed open cost of facilities	Optimal Value
		$\begin{bmatrix} 6 & 10 \\ 3 & 1 \\ 5 & 4 \end{bmatrix}$	{7,7}	21
		$ \begin{bmatrix} 16 & 10 \\ 13 & 5 \\ 4 & 10 \end{bmatrix} $	{17, 17}	42
3×2	14	$\begin{bmatrix} 6 & 10 \\ 3 & 5 \\ 4 & 1 \end{bmatrix}$	$\{27, 27\}$	40
		$\begin{bmatrix} 6 & 20 \\ 3 & 15 \\ 24 & 1 \end{bmatrix}$	$\{10, 15\}$	35
		$\begin{bmatrix} 56 & 10 \\ 23 & 5 \\ 4 & 18 \end{bmatrix}$	$\{27, 10\}$	43

TABLE IV. The Instance 11-Instance 12 of UFLP

TABLE IV. The instance 11-instance 12 of UFLP. $m \times n$ Qubit The service matrix D The set G of fixed open cost of facilities Optimal Va					
	Quon	The service matrix D	The set of three open cost of lacinties	Optimal value	
		$\begin{bmatrix} 16 & 10 \\ 13 & 15 \\ 14 & 10 \\ 15 & 18 \\ 20 & 25 \end{bmatrix}$	{7,7}	82	
5×2	22	2-0 -03			
		$\begin{bmatrix} 16 & 10 \\ 13 & 15 \\ 14 & 10 \\ 15 & 18 \\ 20 & 25 \end{bmatrix}$	{17, 17}	95	

is set to $\sum_{j=0}^{N-1} X_j$. The crucial to the algorithm is the design of the phase separator Hamiltonian, which includes solutions of the UFLP. For the following standard form of the UFLP mathematical model

$$min \quad \sum_{i=1}^{m} \sum_{j=1}^{n} d_{ij} y_{ij} + \sum_{j=1}^{n} g_{j} x_{j}, \tag{B1}$$

s.t.
$$\sum_{j=1}^{n} y_{ij} = 1, \quad i = 1, 2, \dots, m,$$
 (B2)

$$y_{ij} + z_{ij} - x_j = 0, \quad i = 1, \dots, m, j = 1, \dots, n,$$
 (B3)

$$z_{ij}, y_{ij}, x_j \in \{0, 1\}. \tag{B4}$$

To construct phase separator Hamiltonian H_P , we adopt the common method of introducing the hard constraint as a penalty term into the objective function [14–18]. The following unconstrained optimization problem is obtained

$$min \quad \sum_{i=1}^{m} \sum_{j=1}^{n} d_{ij} y_{ij} + \sum_{j=1}^{n} g_j x_j + \lambda \left(\sum_{i=1}^{m} \left(\sum_{j=1}^{n} y_{ij} - 1\right)^2 + \sum_{i=1}^{m} \sum_{j=1}^{n} (y_{ij} + z_{ij} - x_j)^2\right), \tag{B5}$$

where λ is the penalty, determined empirically.

The phase separator Hamiltonian H_P is obtained by replacing binary variables x, y, z in Eq. (B5) with $\frac{I-Z}{2}$

$$H_{P} = \sum_{i=1}^{m} \sum_{j=1}^{n} d_{ij} \frac{I - Z_{n*(i-1)+j-1}}{2} + \sum_{j=1}^{n} g_{j} \frac{I - Z_{m*n+j-1}}{2} + \lambda \left(\sum_{i=1}^{m} \sum_{j=1}^{n} \frac{I - Z_{n*(i-1)+j-1}}{2} - I\right)^{2} + \sum_{i=1}^{m} \sum_{j=1}^{n} \left(\frac{I - Z_{n*(i-1)+j-1}}{2} + \frac{I - Z_{n*(m+i)+j-1}}{2} - \frac{1 - Z_{m*n+j-1}}{2}\right)^{2}\right), (B6)$$

where Z represents Pauli-Z operation and the subscript represents the qubit of action. After the three key points are structured, we apply QAOA to solve the UFLP and perform numerical simulation experiments, and the corresponding 2-layer quantum circuit is shown in Figure 4.

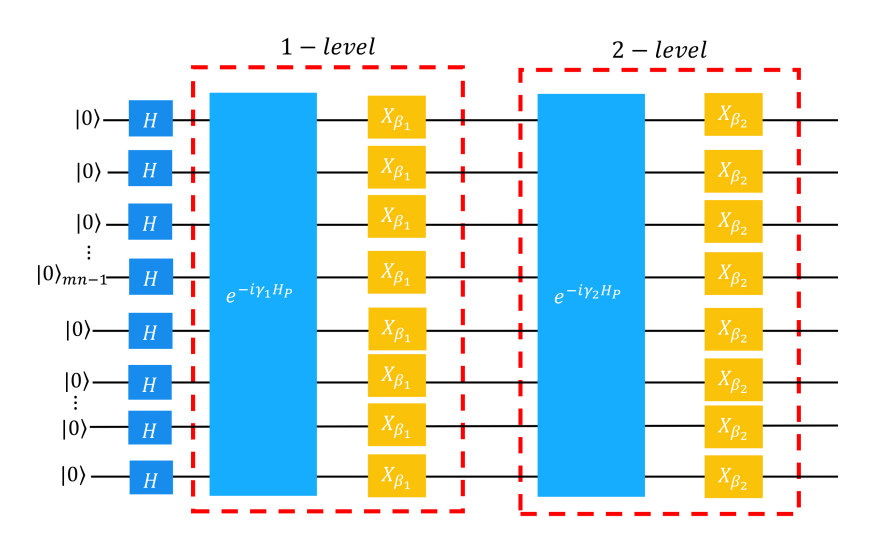


FIG. 4. The overall 2-layer circuit of QAOA.

Appendix C: QAOA+ for UFLP

The crucial points of QAOA+ are the initial state $|x\rangle$, the mixing operators $U(H_M, \beta)$, the phase-separation operators $U(H_P, \gamma)$ for UFLP. For initial state $|x\rangle$, according to Eq. (14), the state

The mixing operators $U(H_M, \beta) = e^{-i\beta H_M}$ depends on Eq. (14) and its structure, and its core is to construct H_M . To maintain the Hamming weight 1 of the constraint Eq. (14), the mixing Hamiltonian H_M is expressed as follows [19, 20]

$$H_M = \sum_{i=0}^{m-1} \sum_{j=0}^{n-2} X_{j+i\cdot n} X_{j+i\cdot n+1} + Y_{j+i\cdot n} Y_{j+i\cdot n+1}, \tag{C1}$$

where X, and Y represents Pauli-X operation, and Pauli-Y operation respectively.

The phase-separation operators $U(H_P, \gamma)$ depends on Eq. (13), and its core is to construct H_P . The objective function $f = \sum_{i=1}^{m} \sum_{j=1}^{n} d_{ij}y_{ij} + \sum_{j=1}^{n} g_j x_j + \lambda \sum_{i=1}^{m} \sum_{j=1}^{n} (y_{ij} + z_{ij} - x_j)^2$, and the phase separator Hamiltonian H_P is obtained by replacing binary variables x, y, z in Eq. (13) with $\frac{I-Z}{2}$

$$H_{P} = \sum_{i=1}^{m} \sum_{j=1}^{n} d_{ij} \frac{I - Z_{n*(i-1)+j-1}}{2} + \sum_{j=1}^{n} g_{j} \frac{I - Z_{m*n+j-1}}{2} + \lambda \sum_{i=1}^{m} \sum_{j=1}^{n} \left(\frac{I - Z_{n*(i-1)+j-1}}{2} + \frac{I - Z_{n*(m+i)+j-1}}{2} - \frac{I - Z_{m*n+j-1}}{2} \right)^{2},$$
 (C2)

where Z represents Pauli-Z operation and the subscript represents the qubit of action. After the three key points are structured, we apply QAOA+ to solve the UFLP and perform numerical simulation experiments, and the corresponding 2-layer quantum circuit is shown in Figure 5.

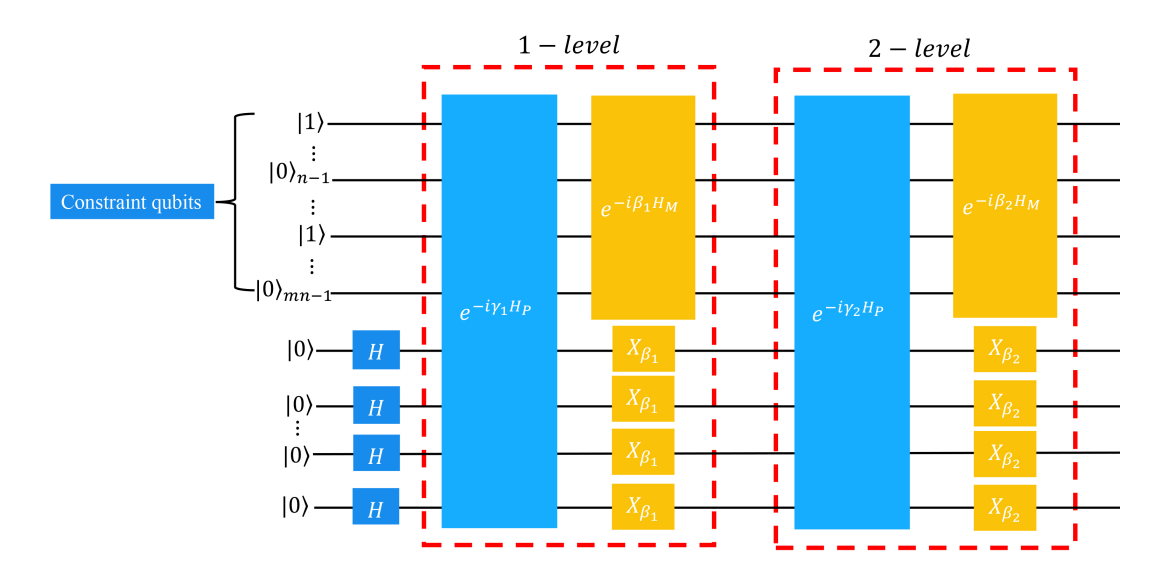


FIG. 5. The overall 2-layer circuit of QAOA+.

Appendix D: Hardware Efficient Ansatz for UFLP

The Hardware Efficient Ansatz (HEA) [13] is a generic name used for ansatzes that are aimed at reducing the circuit depth needed to implement the parametric circuit when using a given quantum hardware. A major advantage of the HEA is its multifunctionality, as it can adapt to encoding symmetries [35, 36] and bring the relevant qubits closer to depth reduction [37], as well as being particularly useful for investigating Hamiltonians similar to the device's interactions [38]. Optimizing the variational parameters of the circuit is performed on classical computers, aiming to find the optimal parameters by minimizing the expected value of the phase separator Hamiltonian. For UFLP, similar to QAOA, the phase separator Hamiltonian is given in Eq. (B6). For Instance 1-Instance 5, the corresponding 2-layer quantum circuit is shown in Figure 6.

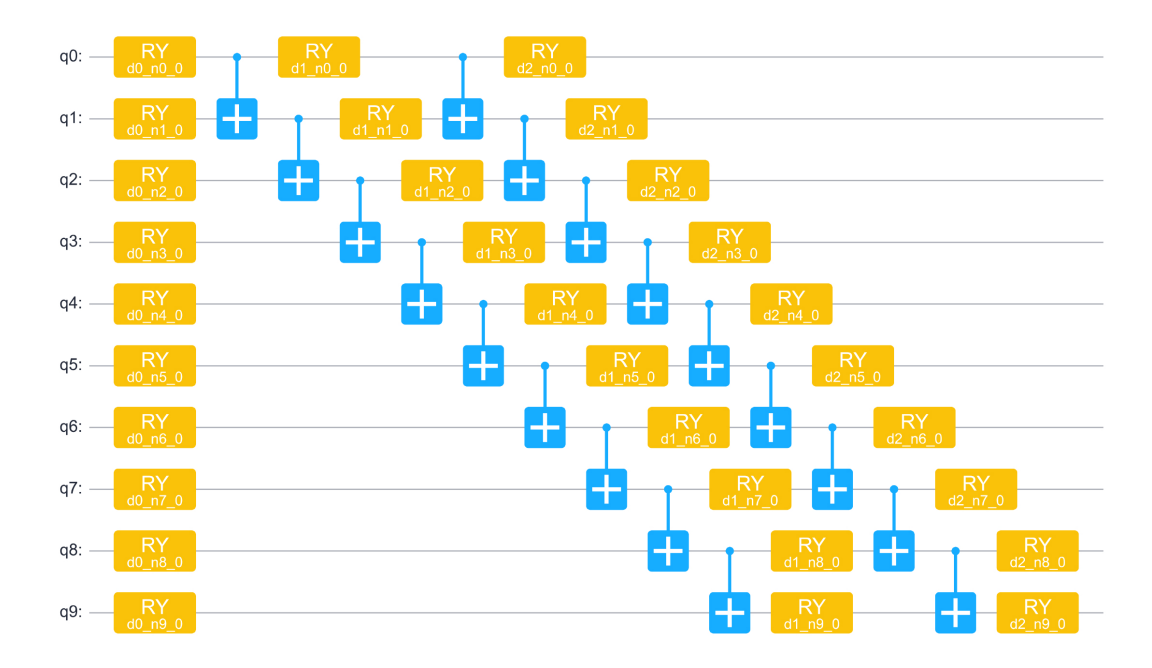


FIG. 6. The overall 2-layer quantum circuit of HEA.